

# A Hierarchical Approach toward Time-Dependent Topographic Visualization

Sagi Dalyot<sup>1</sup>, Yerach Doytsher<sup>2</sup>

<sup>1</sup>Institut für Kartographie und Geoinformatik, Leibniz Universität Hannover, 30167 Hannover, Germany, [sagi.dalyot@ikg.uni-hannover.de](mailto:sagi.dalyot@ikg.uni-hannover.de)

<sup>2</sup>Mapping and Geo-Information Engineering, Technion, Haifa 32000, Israel, [doytsher@technion.ac.il](mailto:doytsher@technion.ac.il)

## ABSTRACT

Visualizing quantitative time-dependent topography changes requires relying on a series of discrete given datasets acquired on a given time-line. The reality of natural physical phenomenon occurring during the acquisition time is complex when trying to mutually model the datasets. Different levels of spatial inter-relations and geometric inconsistencies among the datasets exist. Topographic datasets, such as Digital Terrain Models (DTMs), are non-rigid physical objects that are geometrically different from one another. Any straight forward transition-simulation between these objects will result in a truncated, non-realistic and un-smooth visualization. This research paper suggests adopting a fully automatic hierarchical modeling mechanism implementing several levels of spatial correspondence quantification. These quantification-levels, stored in a geospatial matrix, are utilized for the DTMs transition morphing and blending. Along with designated interpolation concepts this complete process ensures that the visualized transition from one topographic dataset to the other is smooth and continuous while maintaining natural morphological and topological relations.

## 1. INTRODUCTION

Time-dependent visualization of changes in physical entities, such as topography, that presents natural morphologic alterations requires to mutually modeling a series of discrete given datasets. The presumption is that these datasets were acquired on a given time-line and that they represent approximately the same coverage area. Natural physical phenomenon occurring during acquisition times together with existing geometric and morphologic ambiguities add to modeling complexity and different levels of inter-relations and inconsistencies. Commonly used "flip-page" animation method, where each terrain model serves as key-frame, will not suffice (Mach 2007). This is mainly due to the fact that the different topographic datasets are non-rigid objects thus they store different geometric structures and characteristics (differences in level-of-detail (LOD) and resolution, datum ambiguity - to name a few). Any straight forward morphing that ignores preliminary mutual registration and modeling that take into consideration these factors will evidently result in an un-realistic representation and sometimes truncated and un-smooth visualization. This paper introduces a novel hierarchical modeling algorithm that establishes a quantitative multi-level mutual modeling that best describes the geomorphologic changes occurred; thus, enabling to carry out more precise, true-to-nature and realistic morphing visualization. These are essential for a reliable 3D Geographic Information Systems (GIS) workflow, while trying to best describe the reality transition as it occurred. Natural geomorphologic changes can be the outcome of fluvial-, hillslope- and tectonic-processes. Due to the fact that man-made terrain modifications, such as construction work, are fundamentally different from natural geomorphologic ones, it will not be addressed here.

Techniques and methods, which involve the transformation of one object to another object, while creating a continuous transition of shape sequences that changes gradually, are being developed in recent decades on many aspects in the field of Computer Graphics (Stasko 1990). These techniques, best known within the terminology of Shape- Morphing and Blending, attempt to create a natural visual transition effect. The main challenge is establishing algorithms that will be able to match spatially objects that are different from one another with minimal user intervention, while maintaining the properties of objects to maximum extent possible (Thomas 1981). This challenge is intensified when dealing with topographic representations complexities required for virtual-reality GIS and mapping applications. In GIS environments certain aspects are mentioned as basic requirements (Nebiker 2003): modeling complexities; multi- resolution and representation; appearance; animation; simulations; multi-temporal representations, and, topologies and morphologies.

## 2. RELATED WORK

Methods of substitution between objects, i.e., transformation solutions, mainly deal with the problem of correspondence between physical objects. The transformation that is mostly performed is a linear substitution. This is usually carried out for basic-primitives sequence alignment, but still sometimes leads to artifacts, such as collapsing joints and “candy wrapper effect” (Merry 2006). These artifacts are normally caused when a linear blending is implemented while the rotation matrices involved have large angle differences between them. Intuitively, the transformation process should strive to transform objects as “rigidly” as possible, while avoiding distortions by utilizing ‘smart’ solutions rather than a clear linear substitution.

Shape- Morphing and Blending utilize processes in which one object is combined with another object, while trying to stretch, rotate and move it in order to create a maximum matching between them. Two major problems are addressed (Watt 1992):

1. *Vertex Correspondence*, figuring which vertex in one object should blend with another vertex in the other object, such as manual sampling of ‘selection of points’ that define the connectivity between both physical objects;
2. *Vertex Path* (trajectory problem), figuring what path the vertices should take to get from one object space to the other: how to transform the source object points to the destination object points. As stated earlier, the trivial linear transformation is not usually the preferred solution, so more advanced solutions are required, such as including distortions and squinting in the intermediate objects to maintain realistic visualization (Yu 2004; Wang 2007).

Existing concepts and techniques aim at morphing one shape into another shape by concentrating on the shape itself, i.e., trying to stretch, compress and bend one shape into another shape over a given time period and in a realistic fashion (Alexa 2000; Zhang 2008; Stasko 1990). These works are not designed to the GI and mapping scientific disciplines, but rather to real-time virtual reality and animation where usually geometric primitives’ a-priori considerations are made.

## 3. PROPOSED APPROACH

Hierarchical modeling for integration of homogenous DTMs is proposed in the work of Dalyot (2008). A division of the DTMs into several separate homogeneous hierarchical zonal-levels (Figure 1) enables to correctly define the correct localized spatial correspondence, i.e., local transformation parameterization, stored in a registration-matrix. These data-relations are later used for precise DTMs modeling required for reliable integration. The research presented here adopts this concept, adding designed mathematical and geometric considerations aiming at solving the specific problem at hand.

### 3.1 Vertex Correspondence

#### 3.1.1 General Concept

The entire modeled area is divided in both DTMs to congruent frames that are matched via a localized ICP (Iterative Closest Point) algorithm independently and separately. This yields more effective modeling of local random incongruities and trends - quantifying sets of rigid body transformations that align the models ‘best’. ICP matching is accomplished via the minimization of a goal-function based on Least Squares Matching (LSM) of 3D-rigid body transformation: 3-translations  $\{t_x, t_y, t_z\}$ , and 3-rotations  $\{\omega, \phi, \kappa\}$ .

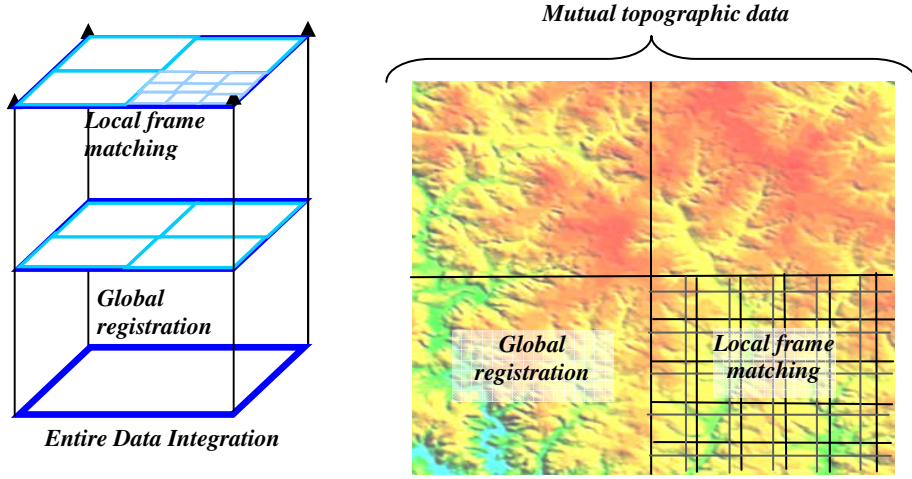


Figure 1: Hierarchical modeling schema, depicting three-working levels.

### 3.1.2 Non-Rigid Constraints

Due to the fact that both DTMs are non-rigid physical bodies, several aspects are considered:

1. Wide-coverage DTMs represent different data-characteristics - namely LOD and resolution - implying that existing ICP homologous points is not explicit;
2. DTMs acquired on different times (epochs) will surely represent different terrain topography and morphology;
3. Data and measurement errors can reflect on the position certainty of points in relatively large scale.

Thus, three geometric constraints are added to the local ICP process, making sure that point-pairs from both DTMs are coupled even if they are not explicitly presented as grid-points. Schematic of this constraints-implementation is depicted in Figure 2. Point  $g(x,y,z)_i$  transformed from  $\text{DTM}_g$  with best available transformation parameters is defined by  $g'(x,y,z)_i$ ; while the counterpart point that exists in  $\text{DTM}_f$  is defined by  $f(x,y,z)_i$ ,  $f(x,y,z)_i$  that is the closest point to  $g'(x,y,z)_i$  validates the three constraints depicted in Equation 1.

$$\begin{aligned}
 z_f &= \frac{Z_1 - Z_0}{D} \cdot x_f + \frac{Z_3 - Z_0}{D} \cdot y_f + \frac{Z_2 - Z_1 - Z_3 + Z_0}{D^2} \cdot x_f \cdot y_f \\
 z_f &= \frac{Z_1 - Z_0}{D} \cdot x_f - \frac{(Z_2 - Z_1 - Z_3 + Z_0) \cdot x'_g}{D^2} \cdot y_f + \frac{Z_2 - Z_1 - Z_3 + Z_0}{D^2} \cdot x_f \cdot y_f + \left( z'_g - \frac{(Z_1 - Z_0) \cdot x'_g}{D} \right) \\
 z_f &= \frac{Z_3 - Z_0}{D} \cdot y_f - \frac{(Z_2 - Z_1 - Z_3 + Z_0) \cdot y'_g}{D^2} \cdot x_f + \frac{Z_2 - Z_1 - Z_3 + Z_0}{D^2} \cdot x_f \cdot y_f + \left( z'_g - \frac{(Z_3 - Z_0) \cdot y'_g}{D} \right)
 \end{aligned} \tag{1}$$

where,  $Z_i$   $\{i \in [0-3]\}$  denotes local DTM grid-cell corner heights (depicted in Figure 2);  $D$  denotes the DTM resolution (slight modifications are required if different resolutions exist for axis/directions, or if Triangulated Irregular Network (TIN) structure of topographic datasets is used).

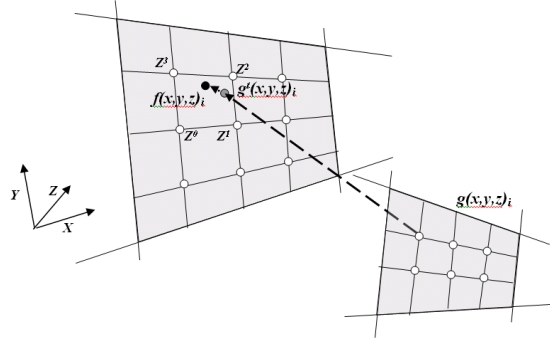
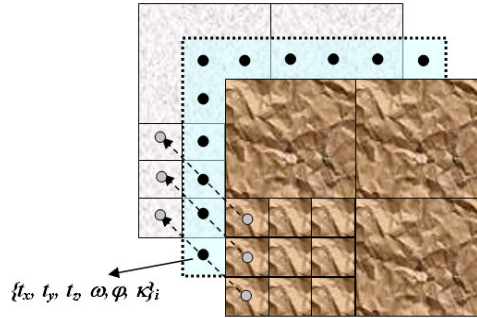


Figure 2: Schematic of Least Squares target function minimization via three constraints.

### 3.2 Vertex Path

The implementation of the localized autonomous ICP matching processes yields the construction of a registration-matrix, a Geo-Database like, depicted in Figure 3. Each matrix node stores the transformation values corresponding to the center of mass for congruent matched frames, i.e., ICP solution:  $\{t_{xj}, t_{yj}, t_{zj}, \phi_j, \kappa_j, \omega_j\}$ . An assumption is made that these values maintain continuity within the matrix coverage area. Hypothetically, when transforming a grid-point from source DTM<sub>g</sub> while using the stored transformation parameters should coincide with the terrain presented by the target DTM<sub>f</sub>. The source-to-target vertex path is a hypothetical morphing between the physical objects regarded as time-dependent one, and any intermediate scene on that path is unique temporal terrain visualization.



**Figure 3:** Transformation matrix (middle) between source and target DTMs. Each matrix-cell stores 6-parameter transformation set.

Two interpolation procedures are pointed required due to resolution differences (matrix vs. DTMs) and the fact that position-derived unique transformation values are required:

1. *Among* the matrix's grid-nodes (*space-domain*). This computation is designed for calculating the position-derived 6-parameters required to transform a grid-point from source to its corresponding position in target;
2. *In-Between* the DTMs (*time-domain*). Spatially, it can be described as if the intermediate terrain is 'situated' in the space between source and target terrains, where this position is derived by the 'time-proportion' and magnitude of the transformations involved. After implementing "*among*" interpolation, an "*in-between*" interpolation is carried out on the resulting values to appreciate spatially the intermediate terrain positioning (time) in that space (source (*time=0*) to target (*time=1*), while  $time \in [0, 1]$ ). All 6-transformation values gradually vary from zero on source DTM, to their maximum value on target DTM.

#### 3.2.1. Translation Values

Interpolating DTM heights using bi-directional third degree parabolic equations is described in Doytsher (1997). This algorithm is an improvement of the simplistic bi-linear area-based interpolation that might produce jagged and unsmooth surface representation. Here, the algorithm handles the three linear characterized translation values stored in the transformation matrix on three separate processes, Equation 2. Implementing this enables to accurately define for each grid-point of the source DTM the 3-translation parameters, and hence to receive a more detailed and smooth 'translation surface'.

$$\begin{aligned}
 F_1(p_n) &= -0.5 \cdot p_n + 1.0 \cdot p_n^2 - 0.5 \cdot p_n^3 \\
 F_2(p_n) &= +1.0 - 2.5 \cdot p_n^2 + 1.5 \cdot p_n^3 \\
 F_3(p_n) &= +0.5 \cdot p_n + 2.0 \cdot p_n^2 - 1.5 \cdot p_n^3 \\
 F_4(p_n) &= -0.5 \cdot p_n^2 + 0.5 \cdot p_n^3
 \end{aligned} \tag{2}$$

$$Z_p = \sum_{i=1}^4 \sum_{j=1}^4 F_j(p_n) \cdot F_i(p_n) \cdot H(i, j)$$

where,  $F_k$  while  $k \in [1-4]$  denotes third-degree parabolic equations;  $Z_p$  denotes calculated value at location  $P$ ,  $p_n$  while  $n \in [x, y]$  denotes normalized inner cell coordinates  $\{0 \leq p_n \leq 1\}$ ;  $H(i, j)$  denotes the values stored in grid-corner points; and  $i, j$  while  $(i, j) \in [1-4]$  denote index of 4x4 neighboring nodes.

### 3.2.2. Rotation Values

Euler angles representation is perhaps the most common parameterization of 3D-orientation space. The interpolation outcome of Euler angles produces a jerky and not continuous motion. The notation of Quaternion, Equation 3, defines a 3-dimensional number system by a 4-dimensional one, where  $W$  is the scalar part, and,  $(X,Y,Z)$  are the vector part with imaginary axes  $i,j,k$ . A practical application of 4D-Quaternions notation is representing 3D-rotations while restricting it to those with unit magnitude. The naïve linear interpolation between two key unit-Quaternions will result in a straight line, which ignores the natural geometry of rotation space in hyper-sphere surface. A geometrical translation results in a great arc drawn between two given key unit-Quaternions, Spherical Linear Interpolation (SLERP), Equation 4, ensuring unique and correct path under all circumstances (Shoemake, 1985).

$$q = W + X \cdot i + Y \cdot j + Z \cdot k \quad (3)$$

$$q_i = SLERP(q_1, q_2, t) = \frac{\sin((1-t) \cdot \theta)}{\sin(\theta)} \cdot q_1 + \frac{\sin(t \cdot \theta)}{\sin(\theta)} \cdot q_2 \quad (4)$$

where,  $q_1$  and  $q_2$  are two unit-Quaternion vectors (orientations);  $\theta$  is the angle between them;  $q_i$  is the resulting unit-Quaternion; and  $t$  is the interpolation magnitude ( $t \in [0, 1]$ ).

SLERP is required for "in-between" interpolation on each given rotation value. A higher order of interpolation is required within a grid-cell, i.e., "among", thus calculating SLERP sequence. This procedure enables the construction of a cubic as a series of three SLERPs of quadrangle of unit-Quaternions on the surface of a 4D-unit hyper-sphere. Shoemake (1985) defines this as Spherical and Quadrangle (SQUAD), Equation 5. Having a grid of four corner-orientations  $\{q_0, q_1, q_2, q_3\}$  a three-step SLERP sequence is implemented. This is equivalent to a Bezier curve with a spherical cubic interpolation. Still, Quaternion multiplication is not a commutative one, so the order in which this SQUAD sequence is implemented should be considered.

$$SQUAD(q_0, q_1, q_2, q_3, t) = SLERP(slerp(q_0, q_1, t), SLERP(q_2, q_3, t), 2t(1-t)) \quad (5)$$

## 4. STATISTICAL ANALYSES

### 4.1 Translation Parameters

Two examples of the suggested bi-directional third degree parabolic interpolation are depicted in Figure 4. The source data is a 700m-resolution transformation matrix and the desired DTM-resolution is 50m. Interpolation for a specific location (i.e., "among") preserved continuity, guaranteeing smooth interpolation and more detailed and continuous translation within the coverage area.

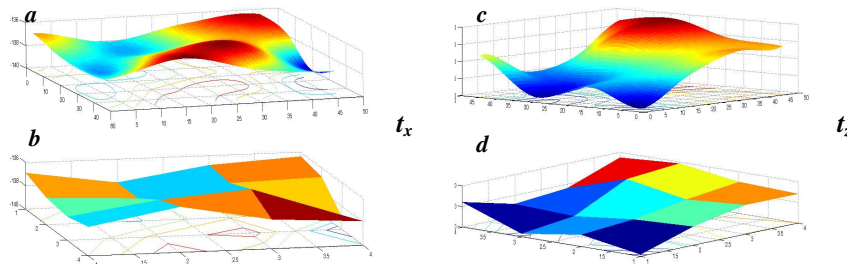


Figure 4: Translation values  $t_x$  and  $t_z$  interpolation: from  $b$  and  $d$  (700m) to  $a$  and  $c$  (50m).

### 4.2. Rotation Parameters

A single matrix cell with rotation values anomalies, depicted in Figure 5, was divided to 121 positions (11x11). After translation to unit-Quaternion parameterization, two SQUAD sequence calculations were implemented. This analysis evaluates whether choosing a specific sequence has an effect on the values calculated. For each position two sets of four unit-Quaternion coefficients values are calculated, later translated to three Euler angles  $(\phi, \kappa, \omega)$ . Figure 6 depicts a surface representing

the resulting 121 three-angle values calculated. It is clear that there are no significant differences in the values: maximum of 0.001 decimal degrees, thus having no significant affect on later processes. The values are smooth and continuous within the entire cell, with no abrupt change in value.

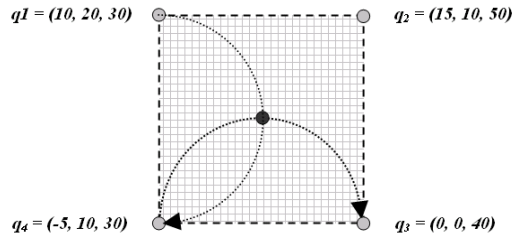


Figure 5: Matrix-cell with two SQUAD sequences (parabola-motion form). Values in degrees.

Figure 7 depicts the value differences between the three angles received via the two SQUAD sequences. Though slight value changes do exist - approximately  $1e^{-03}$  degrees - these values are not significant to have an effect on later processes. The Difference values increase toward the center of the cell, which is a result of the SQUAD and SLERP mathematical notions. Table 1 depicts statistics computed on these differences. It is worth emphasizing that the rotation values usually stored in the matrix are smaller than the ones utilized here. Thus, it can be concluded that utilizing Quaternion space and SLERP and SQUAD interpolation concepts is reliable while producing qualitative results.

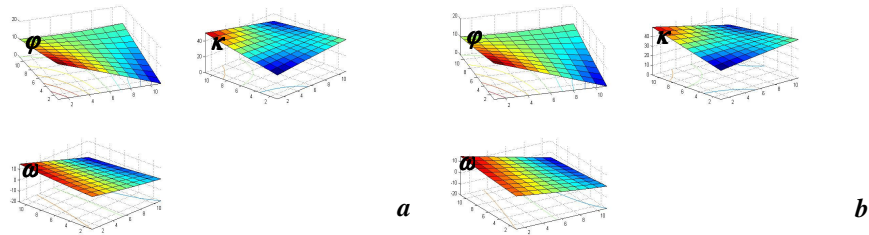


Figure 6: Three Euler angles values calculated via different SQUAD sequences (a,b).

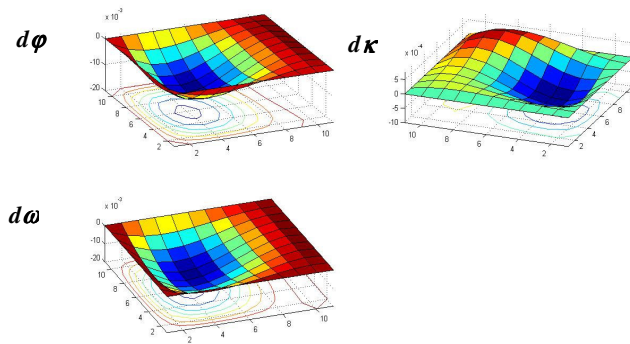
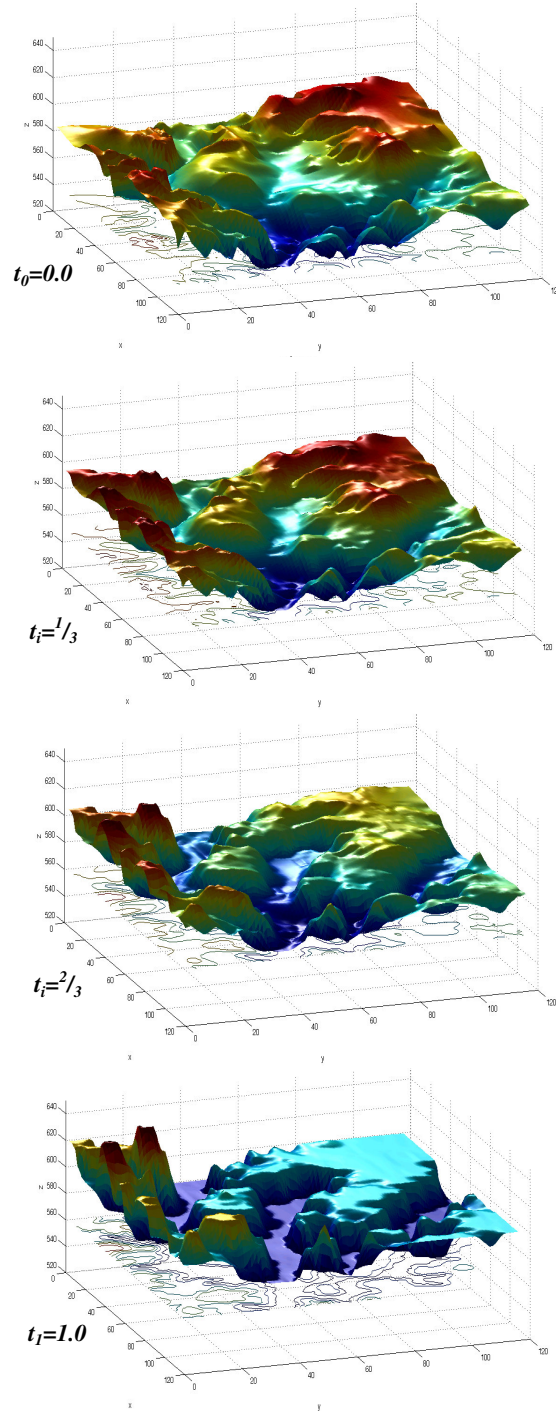


Figure 7: Angular differences calculated via different SQUAD sequences. Values (Z) in degrees.

Table 1: Angular mean and Standard-Deviation (SD) values for the different SQUAD sequences.

Angle [deg]	Mean	SD
$d\varphi$	-0.0033	0.0041
$d\kappa$	0.00005	0.0003
$d\omega$	-0.0042	0.0048

## 5. RESULTS



**Figure 8:** Intermediate scenes  $t_i=1/3$  and  $t_i=2/3$  produced via the hierarchical modeling algorithm (figures with no scale).

Calculation of any hypothetical temporal intermediate position  $t_i$  along the 'vertex path' between DTM 'times' (source  $t_0=0$  and target  $t_1=1$ ) is achieved by using the quantifications stored in the transformation matrix ( $t_i \in [0,1]$ ). The visualization outcome should be true to the geometries exist as well as to natural morphologic alterations occurred. Figure 8 demonstrates scene visualization on two DTMs covering 40km<sup>2</sup>, both with 50m resolution and same level-of-accuracy. Source DTM (top) was produced via photogrammetric means utilizing low resolution satellite imagery, and target DTM (bottom) was produced via digitization of 1:50,000 height contours map. The fully-automatic hierarchical modeling algorithm is implemented, resulting in the modeling of complete different levels of geometric interrelations and correspondence (stored in the transformation matrix). Visualization at 'times'  $t_i=1/3$  and  $t_i=2/3$  is presented - second and third rows. The result presents a natural morphing between the two physical surfaces while overcoming non-realistic artifacts that might occur otherwise. The intermediate scene visualization resembles the geomorphological features existent while transforming and morphing spatially from one surface to another.

A series of intermediate scenes can be produced with  $\Delta t$  interval scenes. Smaller  $\Delta t$  is ( $\Delta t \rightarrow 0$ ) more continuous the transition visualized by the intermediate scenes is. Fusing the scenes results in an animation of all transitions from source-to-target. This can give knowledge regarding hypothetical morphological changes occurred during both epochs (an example with interval of  $\Delta t=0.1$  can be viewed at: <http://www.youtube.com/watch?v=KMjBzIQJwGE>).

## 6. CONCLUSIONS AND DISCUSSION

Standard off-the-shelf GIS and animation applications designed to model topographic datasets mostly rely on the datasets mutual coordinate reference systems, and on simplified geometric set of rules. This is usually in contrast to the physical reality and alterations these datasets model and represent. Shape- Blending and Morphing algorithms will usually require a manual intervention solving the existent complexities.

The proposed hierarchical spatial modeling algorithm - on the other hand - utilizes different level of correlations and interrelations that are a-priori modeled automatically, enabling to quantify phenomenon and tends that are characterized only locally. These qualitative and robust set-of-correspondences are defined as a transformation matrix used for accurate and reliable time-dependent visualization of multi-temporal intermediate scenes. Designated interpolation algorithms ensure correct data-handling of the discrete transformation values, thus enabling continuous geo-oriented simulation analysis to be executed. It is worth noting that this concept is not solely restricted to visualization implementations only, as other various accurate and reliable geo-oriented GIS analyses tasks can utilize from this novel algorithm.

## BIBLIOGRAPHY

- Alexa, M, Cohen-Or, D, Levin, D, 2000. As-Rigid-as-Possible Shape Interpolation, in: Proc. Of the 27th annual International Conference on Computer Graphics and Interactive Techniques, 157-164.
- Dalyot, S, Doytsher, Y, 2008. A Hierarchical Approach Toward 3-D Geospatial Data Set Merging. In: Representing, Modelling and Visualizing the Natural Environment: Innovations in GIS 13, CRC Press, Taylor & Francis Group, 195-220.
- Doytsher, Y, Hall, JK, 1997. Interpolation of DTM using Bi-Directional Third-Degree Parabolic Equations, with FORTRAN Subroutines, Computers and Geosciences, 23(9):1013-1020.
- Mach, R, Petschek, P, 2007. Visualization of Digital Terrain and Landscape Data: A Manual, Springer, 1<sup>st</sup> edition.
- Merry, B, Marais, P, Gain, J, 2006. Animation space: A truly linear framework for character animation, ACM Trans. Graph., 25.
- Nebiker, S, 2003. Support for visualisation and animation in a scalable 3D GIS environment: motivation, concepts and implementation. International Archives of the Photogrammetry, Remote Sensing and Spatial Information Sciences, Vol. XXXIV-5/W10.



## A Hierarchical Approach toward Time-Dependent Topographic Visualization

- Shoemake, K, 1985. Animating Rotation with Quaternion Curves, International Conference on Computer Graphics and Interactive Techniques, 19(3):245-254.
- Stasko, JT, 1990. The Path-Transition Paradigm: a Practical Methodology for Adding Animation to Program Interfaces, Journal of Visual Languages and Computing, 1(3):213-236.
- Thomas, F, Johnston, O, 1981. Disney Animation: The Illusion Of Life, Abbeyville Publishers, NY.
- Wang, R, Pulli, K, Popovi, J, 2007. Real-time enveloping with rotational regression, ACM Trans. Graph., 26(3):73.
- Watt A, Watt M, 1992. Advanced Animation and Rendering Techniques, ACM, New-York, USA.
- Yu, Y, Zhou, K, Xu, D, Shi, X, Bao, H, Guo, B, Shum, HY, 2004. Mesh Editing with Poisson-based Gradient Field Manipulation, ACM Transactions on Graphics (TOG), 23(3):644-651.
- Zhang, H, Sheffer, A, Cohen-Or, D, Zhou, Q, van Kaick, O, Tagliasacchi, A, 2008. Deformation-Driven Shape Correspondence, Proc. Symposium on Geometry Processing, 27(5):1431-1439.